Simultaneous analysis of stable and radiogenic strontium isotopes in reference materials, plants and modern tooth enamel

Danaé Guiserix, Emmanuelle Albalat, Henriette Ueckermann, Priyanka Davechand, Linda Iaccheri, Grant Bybee, Shaw Badenhorst, Vincent Balter

Simultaneous analysis of stable and radiogenic strontium isotopes in reference materials, plants and modern tooth enamel

Danaé Guiserix [a], Emmanuelle Albalat [a], Henriette Ueckermann [b], Priyanka Davechand [c], Linda M. Iaccheri [c], Grant Bybee [c], Shaw Badenhorst [d], Vincent Balter [a]

[a] CNRS UMR 5276, LGLTPE, Univ. Lyon, ENS de Lyon, Univ. Lyon 1, 46 Allée d'Italie, 69342, Lyon Cedex 07, France

[b] Department of Geology, University of Johannesburg, Auckland Park 2006, South Africa

[c] School of Geosciences, University of the Witwatersrand, 1 Jan Smuts Avenue, Braamfontein, Johannesburg 2000, South Africa

[d] Evolutionary Studies Institute, University of the Witwatersrand, Private Bag 3, Wits 2050, South Africa

Abstract

Radiogenic strontium isotopes ($^{87}Sr/^{86}Sr$) are a useful tool in forensics, ecology, bioarcheology and paleoanthropology allowing investigation of present and past migration and landscape use. The measurement of the $^{87}Sr/^{86}Sr$ ratio traditionally assumes a constant stable ($^{88}Sr/^{86}Sr$) isotope ratio. However, some studies indicate that these stable Sr isotopes may display mass-dependent fractionation, suggesting that the $^{88}Sr/^{86}Sr$ ratio may fingerprint previously unknown dietary and physiological information. Here we present a survey of the variability of $\delta^{88}Sr$ values, along with the $^{87}Sr/^{86}Sr$ ratios, in fourteen reference materials of geological and biological origin using MC-ICPMS. The measurements employ a simple sample-standard bracketing method and zirconium external correction. Comparisons with double-spiked $\delta^{88}Sr$ TIMS analyses show a very good agreement (0.014 ‰; n = 10). We then applied this method to explore the fractionation of the $^{88}Sr/^{86}Sr$ ratio in tooth enamel of mammals from two modern food-chains (Kruger National Park and Western Cape, South Africa), and from modern South African chacma baboon populations. Clear differences in the $\delta^{88}Sr$ values are observed between plants and teeth of herbivores (~ -0.26 ‰; n=5), but the distinction between herbivores and carnivores requires further investigation. Variations between tooth enamel of young and adult baboons suggests that the $\delta^{88}Sr$ is a promising indicator of weaning behaviors. Our method implementation and preliminary results highlight the importance of coupled radiogenic and stable Sr isotope determination in extant and extinct vertebrates.

Keywords

Non-traditional isotopes, stable strontium isotopes, radiogenic strontium isotopes, trophic chain, weaning

1. Introduction

There are four naturally occurring strontium (Sr) isotopes, all of which are stable (^{84}Sr, ^{86}Sr, ^{88}Sr, ^{87}Sr), but one, ^{87}Sr, is the radiogenic product of the β-decay radioactivity of rubidium-87 (^{87}Rb; half-life = 48.8 Ga). Given that the atomic properties of Sr are similar to those of calcium (Ca), Sr is incorporated into the body as a Ca substitute, undergoing discrimination processes that lower the Sr/Ca ratio during metabolic processes involving Ca (Balter, 2004). Multi-collector inductively-coupled plasma mass spectrometers (MC-ICPMS) and thermal ionization mass spectrometers (TIMS), which are routinely used for the measurements of the $^{87}Sr/^{86}Sr$ ratio, induce an instrumental mass-bias during measurement that needs to be corrected, thus the true $^{86}Sr/^{88}Sr$ ratio is traditionally set at 0.1194 to correct the mass-bias on the $^{87}Sr/^{86}Sr$ ratio. The $^{87}Sr/^{86}Sr$ ratio in the body of an animal records that of the soil/substrate on which the animal lives (Price et al., 2002; Lazzerini et al., 2021). By measuring the $^{87}Sr/^{86}Sr$ ratio in tissues forming at different periods of life, such as bone and tooth enamel, or within tooth enamel using laser ablation, it is possible to reconstruct the mobility and range of the animal, with reference to the Sr isotope ratio of the substrate (Knudson et al., 2004; Martin et al. 2016,Sillen and Balter, 2018).

55 However, with the improvement of MC-ICPMS precision in the last twenty years,
56 variations of the $^{88}Sr/^{86}Sr$ ratio have been increasingly scrutinized in geological materials
57 since the first measurement of that ratio in seawater (Fietzke and Eisenhauer, 2006).
58 Variations of this ratio relative to the international standard NIST SRM-987 are expressed
59 as $\delta^{88/86}Sr_{SRM987}$, defined as following:

60 $$\delta^{88/86}Sr_{SRM987} = (\frac{^{88}Sr/^{86}Sr_{\text{sample}}}{^{88}Sr/^{86}Sr_{\text{NIST SRM987}}} - 1) \times 1000$$

61 The classical and shorter notation $\delta^{88}Sr$ will be used in the following text. There is only
62 scarce data concerning the $\delta^{88}Sr$ value in biological materials. Recent studies suggest that
63 stable Sr isotopes in bone and tooth enamel may be a good indicator of paleodietary range
64 and trophic level (Knudson et al., 2010; Lewis et al., 2017; Brazier et al., 2019). Indeed, ^{86}Sr
65 seems to be preferentially incorporated into biological system compared to ^{88}Sr. Analyses of
66 plants show preferred uptake of ^{86}Sr relative to ^{88}Sr in the nutrient pathways leading to
67 lighter isotopic signatures in leaves than in roots and soil (de Souza et al., 2010; Liu et al.,
68 2016; Guibourdenche et al., 2020). Up trophic chains, the Sr isotope fractionation remains
69 poorly studied, but it is already noticeable that all $\delta^{88}Sr$ values in plants are positive (de
70 Souza et al., 2010; Liu et al., 2016; Hajj et al., 2017; Brazier et al., 2019), while all $\delta^{88}Sr$
71 values in terrestrial animals are negative (Knudson et al., 2010; Lewis et al., 2017; Brazier
72 et al., 2019), relative to the SRM-987 standard. In a controlled feeding study on pigs, a shift
73 of -0.32 ‰ from diet to dental enamel has been observed (Lewis et al., 2017), consistent
74 with the plant data. Different methods have been developed in order to overcome
75 instrumental mass bias during measurements of the $^{88}Sr/^{86}Sr$ and $^{87}Sr/^{86}Sr$ ratios. Analyses
76 with a TIMS use a $^{84}Sr/^{86}Sr$ double spike to correct for the instrumental mass bias

(Krabbenhöft et al., 2009; Neymark et al., 2014; Charlier et al., 2017; Lewis et al., 2017; Brazier et al., 2019) and is the method of reference to achieve the best precision (between 0.01 and 0.02 ‰ (Brazier et al., 2019)). Measurement method using a MC-ICPMS includes sample-standard bracketing method (SSB) (Fietzke and Eisenhauer, 2006; Ma et al., 2013) and correction using a zirconium (Zr) internal standard (Ohno and Hirata, 2007; Liu et al., 2012, 2016, 2017; Xu et al., 2020). Both methods can be used simultaneously (Irrgeher et al., 2013; Liu et al., 2017; Argentino et al., 2021).

A combination of these two methods is used in the present study and we test the procedure on fourteen reference materials with various mineral and biological matrices. The robustness and accuracy of this method was assessed in different laboratories. In South Africa sample preparation was done at the Wits Isotope Geoscience Laboratory (WIGL, University of the Witwatersrand, Johannesburg, South Africa), while the analytical measurements were done at the University of Johannesburg (UJ, Johannesburg, South Africa). Further work was achieved at the Laboratoire de géologie de Lyon (LGLTPE, Ecole Normale Supérieure de Lyon, France). In addition to the reference materials, we also measured the $^{88}Sr/^{86}Sr$ and $^{87}Sr/^{86}Sr$ ratios in animal and plant samples from extant ecosystems in South Africa to provide a first overview of the Sr stable isotope systematics in modern ecosystems and to challenge the possible use as a paleodietary indicator.

2. Material and methods

2.1. Reference material description

Eleven reference materials with known $^{88}Sr/^{86}Sr$ and $^{87}Sr/^{86}Sr$ ratios (biological matrix: SRM-1400, SRM-1486, BCR-380R, BCR-383 and SRM-1570a; geological matrix: JC-p1, UB-N, BHVO-2, BCR-1, and GS-N; seawater: IAPSO) and three reference materials with unknown $^{88}Sr/^{86}Sr$ and $^{87}Sr/^{86}Sr$ ratios (geological matrix: Granite GA, NBS-120c and SRM-915b) were analyzed in both labs. The descriptions of the standards are provided in Table 1. Reference material aliquots were weighed to reach around 5 µg of Sr.

Table 1: Description of the reference materials analyzed in this study

Reference material	Description	Sr (µg.g^{-1})
Animal		
BCR-380R	Whole milk powder	2.72
NIST SRM 1400	Cow bone ash powder	249
NIST SRM 1486	Cow bone meal powder	264
Vegetal		
BCR-383	Green bean powder	5.26
NIST SRM 1570a	Spinach powder	55
Carbonate		
JC-p1	Coral powder (*Porites sp.*)	6896
NIST SRM 915b	Calcium carbonate	150
Sea water		
IAPSO	North Atlantic sea water	7.9
Crustal and mantle rocks		
UB-N	Serpentinite powder	9
BHVO-2	Basalt powder	389
BCR-1	Basalt powder	330
GS-N	Granite powder	570
Granite GA	Granite powder	310
NIST NBS 120c	Phosphate rock powder	840

2.2. Sample description

We also measure $^{88}Sr/^{86}Sr$ and $^{87}Sr/^{86}Sr$ ratios in two sets of modern samples. The first set of samples are from tooth enamel collected from modern chacma baboon (*Papio ursinus*) skulls provided by the Ditsong National Museum of Natural History (Pretoria, South Africa). Teeth were extracted from sixteen skulls of chacma baboons from a reserve in Calitzdorp (Western Cape, South Africa). Details for baboons and the geographical context are available in a previous study (Brand, 1994). The list of sampled individuals is presented in Table S1. The first molar of the upper jaw was sampled in 4 adults (over 6 years old) and 3 sub-adults (around 3 years old). Deciduous teeth (milk incisor, molar and canine) from 8 sub-adult baboons and the third molar from an adult were also sampled. All the teeth were washed with distilled water before drilling and the surfaces were cleaned with an abrasive drill bit. Sampling was located in the mesio- or distobuccal cusps of the teeth, and drilled using a bit diameter of 0.8 mm. Only the enamel was sampled to avoid contamination with dentine. Between 5 and 10 mg of powder was recovered. This set of material has been analyzed at UJ, using the WIGL-UJ method. The second set of samples consists in tooth enamel of herbivores and carnivores from the Kruger National Park (KNP) and Western Cape (WC), in South Africa. Details for sex, age and geographical context of these specimens are given in Table S2. The teeth were cleaned with distilled water before sampling. Plant residues trapped in the dentition of herbivorous mammals were also collected. The samples were stored at the Ditsong National Museum of Natural History (Pretoria, South Africa). They were prepared and analyzed at the LGLTPE, using the LGLTPE-2 analytical method. Around 5 mg of enamel powder was sampled, and the same quantity was taken from plant residues.

2.3. Sample digestion

WIGL

All sample preparation procedures were carried out in a Class 100 clean room under laminar flow hoods. Organics present in biological samples were removed via an oxidative digestion procedure. Thus 2 mL of concentrated HNO_3 (14M) and 0.5 mL of H_2O_2 (30 %) were added to SRM-1400 and SRM-1486, but also to evaporated IAPSO and baboon tooth enamel. Beakers were then left on a hotplate for three days at 110 °C. They were opened at regular 10 minutes intervals during the first hours to allow degassing. The BHVO-2 standard was dissolved using 2 mL of concentrated HNO_3 (14M) and 1 mL concentrated HF. The closed beakers were left on a hotplate (110 °C) for 48h. After complete dissolution all the samples were dried down and subsequently taken up with 1 mL of HNO_3 (3M).

LGLTPE

Sample preparation procedures at the LGLTPE were carried out in a clean room under laminar flow hoods. All the acids used were purified twice by sub-boiling distillation. As at the WIGL, 4 mL concentrated HNO_3 (15M) and 1 mL H_2O_2 (30 %) were added to standards containing organics (i.e., BCR-383, BCR-380R, SRM-1486, SRM-1400 and SRM-1570a), but also to IAPSO and JC-p1, and closed beakers were left on a hotplate (110 °C) for 48h. They were unscrewed regularly to allow degassing. Tooth enamel samples and plant residues from the KNP and WC were dissolved using the same protocol. The SRM-915b and NBS-120c standards were dissolved in 1 mL concentrated HNO_3 (15M) and centrifuged to remove potential silicate particles. All rock samples (i.e., UB-N, BHVO-2, BCR-1, GS-N and

Granite GA) were digested using 2 mL concentrated HNO_3 (15M) and 1 mL concentrated HF. Closed beakers were left on the hotplate (110 °C) for 48h and evaporated to dryness, taken up with 6N HCl and a few drops of $HClO_4$ and evaporated on a hotplate (120 °C) to eliminate fluorides. This last step was repeated until all fluorides were dissolved. After, digestion all the samples were dried down and redissolved in 1 mL of 3M HNO_3.

2.4. Sample preparation and instrumentation

WIGL

Isotopic measurements of Sr in biological and geological samples require the separation of Sr from the matrix with a special attention to avoid any isobaric interference with ^{87}Rb and Zr contamination. Strontium must be recovered quantitatively after the chromatographic separation to ensure the absence of any chemical isotopic mass fractionation during matrix and Sr elutions. The column chemistry protocol set up at WIGL was inspired by that of Tacail et al. (Tacail et al., 2014) and De Muynck et al. (De Muynck et al., 2009). Both protocols use the Sr spec™ resin (TrisKem International). 300µL of Sr spec™ resin is loaded into 2 mL polypropylene columns. The elution protocol is given in Table 2. The resin is discarded after a single use.

Table 2: Ion exchange protocols for the chromatographic separation of Sr

Lab	WIGL	LGLTPE
Wash	4 mL 0.5M HNO_3	4 mL 0.5M HNO_3
Conditioning	2.5 mL 3M HNO_3	2.5 mL 3M HNO_3
Load sample	1 mL 3M HNO_3	1 mL 3M HNO_3
Matrix elution	2.5 mL 3M HNO_3	3.5 mL 3M HNO_3
Sr elution	16 mL 0.5M HNO_3	7 mL 0.005M HNO_3

UJ

The isotopic analyses were performed on a Nu Plasma II (Nu Instrument) MC-ICPMS at UJ. The SRM-987 was used as the isotopic reference standard for Sr. On the day of the analysis session, samples and standards were diluted with 0.05M HNO_3 to reach a concentration of 500 µg.L^{-1}, leading to a typical intensity of 8 V in the H1 collector (^{88}Sr). A high purity Zr solution (Alfa Aesar, 1000 ppm) was diluted and added to the standard and sample solutions at 500 µg.L^{-1}. The true ratio of ^{91}Zr/^{90}Zr is 0.218126 according to the commission on isotopic abundances IUPAC (Meija et al., 2016). Measurements were carried out in static mode and a single measurement consisted of one block of 40 cycles with an integration time of 10 s. Daily calibration was performed to optimize operating conditions for maximum Sr and Zr signal stability, which was monitored with repeated measurements on SRM-987. The instrument settings are given in Table 3.

Table 3: Instrument settings and data acquisition parameters for MC-ICP-MS analysis, and main differences between the three measurement methods

Method	**UJ**	**LGLTPE-1**	**LGLTPE-2**
Element (+internal standard)	Sr(+Zr)	Sr(+Zr)	Sr(+Zr)
MC-ICP-MS	Nu Plasma II	Nu Plasma 500	Nu Plasma 500
RF power (W)	1300	1350	1350
Plasma condition	wet, cyclonic spray chamber	idem	idem
Coolant Ar flow ($L.min^{-1}$)	13.00	13.00	13.5
Auxiliary Ar flow ($L.min^{-1}$)	0.80	1.46	1.80
Nebulizer Ar flow ($L.min^{-1}$)	34.50	37.9	35.1
Mass resolution	300	300	300
Cup configuration	H6: ^{91}Zr; H5: ^{90}Zr H1: ^{88}Sr; L1: ^{87}Sr L3: ^{86}Sr; L5: ^{85}Rb L6: ^{83}Kr; L7: ^{82}Kr	H6: ^{91}Zr; H5: ^{90}Zr H2: ^{88}Sr; Ax: ^{87}Sr L2: ^{86}Sr; L3: ^{85}Rb L4: ^{84}Sr; L5: ^{83}Kr	H6: ^{92}Zr; H5: ^{91}Zr H4: ^{90}Zr; Ax: ^{88}Sr L2: ^{87}Sr; L3: ^{86}Sr L4: ^{85}Rb; L5: ^{84}Sr
Sensitivity	^{88}Sr 0.5 ppm: 8V	^{88}Sr 0.3 ppm: 8V	^{88}Sr 0.3 ppm: 8V

Integration time (s)	10	10	10
Cycles	40	40	20
Isotope ratio used for mass bias correction of $^{88}Sr/^{86}Sr$	$^{91}Zr/^{90}Zr$	$^{91}Zr/^{90}Zr$	$^{92}Zr/^{90}Zr$ and $^{91}Zr/^{90}Zr$
Baselines	On-peak zero	Deflected beam	On-peak zero
Blank signal	$2.7*10^{-3}$ V	$3.5*10^{-3}$ V	$3.5*10^{-3}$ V
Kr interference correction	None	Yes	None
Rb interference correction	Yes	Yes	Yes

189

190 *Interference correction*

191 Krypton (Kr) contamination of argon (Ar) gas may interfere with ^{86}Sr. Measurement
192 background was determined at the start of each measurement session by analyzing a 0.05M
193 HNO_3 laboratory blank. The on-peak background intensities were subtracted from the
194 measurement signals during measurement, correcting for possible Kr interference.
195 To calculate the $^{87}Sr/^{86}Sr$ values, the isobaric interference of ^{87}Rb on ^{87}Sr was corrected
196 following the equation:

$$^{87}Rb = Meas(^{85}Rb) \times Ref(^{87}Rb/^{85}Rb) \times \left(\frac{M(^{87}Rb)}{M(^{85}Rb)}\right)^{Fract_{Sr}} \quad \{1\}$$

197

$$^{87}Sr = Meas(^{87}Sr) - ^{87}Rb \quad \{2\}$$

198

199 With *Meas(^{85}Rb)* and *Meas(^{87}Sr)* being the measured intensity at mass 85 and 87,
200 respectively, and *M(^{87}Rb)* and *M(^{85}Rb)* corresponding to Rb isotopic masses. *Ref($^{87}Rb/^{85}Rb$)*
201 is the natural abundance ratio extracted from the latest IUPAC report (0.3856, (Meija et al.,
202 2016)). $Fract_{Sr}$ is the fractionation factor defined as in equation 3 that can be used to
203 correct for Rb interferences as long as the Rb concentration in the sample is small (Ehrlich

et al., 2001). The average measured intensity of mass 85 in the samples was $2*10^{-05}$ V, which is negligible compared to the intensity measured on mass 87 (0.7 V).

Normalization of $^{87}Sr/^{86}Sr$ ratio

The $^{87}Sr/^{86}Sr$ ratio was obtained according to classic calculations (Marisa Almeida and D. Vasconcelos, 2001). The instrumental mass bias is evaluated by the fractionation factor $Fract_{Sr}$, calculated using Russel's exponential law (Russell et al., 1978):

$$Fract_{Sr} = \frac{Ln\left(\frac{True(^{86}Sr/^{88}Sr)}{Meas(^{86}Sr/^{88}Sr)}\right)}{Ln\left(\frac{M(^{86}Sr)}{M(^{88}Sr)}\right)} \quad \{3\}$$

$M(^{88}Sr)$ and $M(^{86}Sr)$ correspond to Sr isotopic masses and $True(^{86}Sr/^{88}Sr)$ equals 0.1194 (Meija et al., 2016). This fractionation factor can then be used to normalize the $^{87}Sr/^{86}Sr$ ratio:

$$Norm(^{87}Sr/^{86}Sr) = Meas(^{87}Sr/^{86}Sr) \times \left(\frac{M(^{87}Sr)}{M(^{86}Sr)}\right)^{Fract_{Sr}} \quad \{4\}$$

However, the mass bias may change during the analytical session. Thus, a sample-standard bracketing method (SSB) was applied to take these variations into account, using the equation:

$$(^{87}Sr/^{86}Sr)_{sample} = Norm(^{87}Sr/^{86}Sr)_{sample} \times \frac{Ref(^{87}Sr/^{86}Sr)_{SRM987} \times 2}{Norm(^{87}Sr/^{86}Sr)_{stdA} + Norm(^{87}Sr/^{86}Sr)_{stdB}} \quad \{5\}$$

With $Norm(^{87}Sr/^{86}Sr)_{std}$ being the measured and normalized $^{87}Sr/^{86}Sr$ ratios of the previous (A) and following (B) standards. $Ref(^{87}Sr/^{86}Sr)_{SRM987}$ is the "true" $^{87}Sr/^{86}Sr$ value of the NIST SRM-987, set at 0.71024. Although NIST certifies the SRM-987 reference material $^{87}Sr/^{86}Sr$ value at 0.71034 ± 0.00026, previous studies have rather been measuring and using a value of 0.71024, which falls inside the uncertainties of the certified value. This difference may be explained using 0.1194 as the true $^{86}Sr/^{88}Sr$, instead of the true value of this standard (0.119352). For the sake of comparison with other studies (e.g. Weber et al., 2018; Brazier et al., 2019), it was decided to use in the present study a SRM-987 $^{87}Sr/^{86}Sr$ value of 0.71024 as the bracketing standard value.

As the measurement method proposed here allows the measurements of the stable $^{88}Sr/^{86}Sr$ ratio corrected from the mass bias and the normalized radiogenic $^{87}Sr/^{86}Sr$ ratio simultaneously, it is possible to use the Zr-corrected $^{86}Sr/^{88}Sr$ ratio of a sample to normalize its $^{87}Sr/^{86}Sr$ ratio. However, the $^{87}Sr/^{86}Sr$ value in a biological sample obtained after normalization to a constant $^{86}Sr/^{88}Sr$ ratio of 0.1194 can solely correspond to the initial $^{87}Sr/^{86}Sr$ ratio i.e., that of the substrate, which depends ultimately on ^{87}Rb radioactive disintegration. This constitutes the methodological ground on which are based provenance and mobility studies. Taking these considerations into account and for the sake of comparison with previous work, in this study we decided to present only the $^{87}Sr/^{86}Sr$ ratio normalized with a constant $^{86}Sr/^{88}Sr$ ratio of 0.1194. A comparison of those two corrections through three analytical sessions can be found in Figures S1 (Supplementary material) showing, as expected, a strong correlation with a 1:1 slope.

Correction of the $^{88}Sr/^{86}Sr$ ratio

Given that Zr and Sr have very similar masses, instrumental mass fractionation does not vary independently for both elements (Maréchal et al., 1999). Therefore, the Zr fractionation factor can then be used to correct $^{88}Sr/^{86}Sr$ using Russel's exponential law (Russell et al., 1978). The measured $^{91}Zr/^{90}Zr$ ratio is used to calculate the fractionation factor of the instrument ($Fract_{Zr}$) using the equation:

$$Fract_{Zr} = \frac{Ln\left(\frac{True(^{91}Zr/^{90}Zr)}{Meas(^{91}Zr/^{90}Zr)}\right)}{Ln\left(\frac{M(^{91}Zr)}{M(^{90}Zr)}\right)} \quad \{6\}$$

With $M(^{91}Zr)$ and $M(^{90}Zr)$ corresponding to Zr isotopes isotopic masses. The stable isotopic composition of Sr is then corrected using the equation:

$$Corr(^{88}Sr/^{86}Sr) = Meas(^{88}Sr/^{86}Sr) \times \left(\frac{M(^{88}Sr)}{M(^{86}Sr)}\right)^{Fract_{Zr}} \quad \{7\}$$

We also apply the sample-standard bracketing method (SSB) to correct for the instrumental mass-bias variations during the measurement session. The sample $\delta^{88}Sr$ value is calculated using the $^{88}Sr/^{86}Sr$ ratio averaged from the previous (A) and the following (B) standard:

$$\delta^{88}Sr = \left(\frac{Corr(^{88}Sr/^{86}Sr)_{sample} \times 2}{Corr(^{88}Sr/^{86}Sr)_{stdA} + Corr(^{88}Sr/^{86}Sr)_{stdB}} - 1\right) \times 1000 \quad \{8\}$$

This standard must have known Sr isotopic composition. Special care was given to closely match the concentration between the bracketing standard (SRM-987) and the samples (Ma

et al., 2013; Liu et al., 2016). The co-variation between Sr and Zr can be observed in Figures S2 and S3, showing the drift of the non-corrected $^{92}Zr/^{90}Zr$ and $^{88}Sr/^{86}Sr$ ratios in SRM-987 through an analytical session.

LGLTPE

Strontium was isolated from the matrix using a protocol similar to that set-up at WIGL with identical resin volume and size column, however the acid molarity for the Sr elution was slightly modified to reduce acid consumption. As shown in Table 2, Sr is eluted with 7 mL of 0.005M HNO_3. A small aliquot (15µL) was saved before and after the elution protocol for the quantitative determination of Sr and other trace element concentrations.

The measurement of Sr, Rb and Zr concentrations was performed on a quadrupole ICPMS (Thermo Scientific, iCap-Q) using the ^{85}Rb, ^{88}Sr and ^{90}Zr masses. Aliquots were diluted in 5 mL of 0.5M HNO_3 with 2 $\mu g.L^{-1}$ rhodium (Rh) as an internal standard. Strontium recovery from the chromatographic separation was found to be 95.5 ± 6% (2SD, n=24), suggesting quantitative yields and therefore absence of any mass-dependent fractionation. The low amount of Sr in procedural blanks (between 1 and 4 ng) was typically 0.04 % of total Sr in the samples. After the chromatographic separation of Sr, the Sr/Zr ratio was > 100 on average.

Isotopic analyses were performed on a Nu Plasma 500 MC-ICP-MS (Nu Instruments). On the day of the measurement session, samples and standards were diluted with 0.05M HNO_3 to reach a Sr concentration corresponding to an intensity of 8 V in the H2 collector (^{88}Sr) (usually 250 or 300 $\mu g.L^{-1}$). The solutions were then doped with a high purity Zr solution (Alfa Aesar) to reach a $^{90}Zr/^{88}Sr$ close to unity. Measurements were carried out in

static, multi collection mode and one single measurement consisted in one block of 40 cycles with an integration time of 10 s. Electronic zero by ESA deflection were subtracted online on each measurement. Krypton possible contribution was monitored by measuring the intensity at mass 83 (^{83}Kr) and subtracting its influence on mass 86:

$$^{86}Kr = Meas(^{83}Kr) \times Ref(^{86}Kr/^{83}Kr) \quad \{9\}$$

$$^{86}Sr = Meas(^{86}Sr) \; - ^{86}Kr \quad \{10\}$$

With $M(^{86}Kr)$ and $M(^{83}Kr)$ corresponding to Kr isotopic masses. $Ref(^{86}Kr/^{83}Kr)$ (1.50) is the ratio of Kr isotopes natural abundances extracted from the latest IUPAC report (Meija et al., 2016). The isobaric interference of ^{87}Rb on ^{87}Sr was corrected using equations {1} and {2}. The typical intensity on mass 85 (^{85}Rb) for the samples was $2*10^{-4}$ V which is low enough to use the correction, with a measured intensity of 0.7 V on mass 87. The ^{87}Sr/^{86}Sr ratio was normalized using equations {3} and {4} and the instrumental induced mass-bias on ^{88}Sr/^{86}Sr was corrected using equations {6} and {7}. SSB was also applied using equation {8}. This analytical method is indicated as LGLTPE-1.

A second analytical method was tested at LGLTPE, indicated as LGLTPE-2 in Table 3. This method used an on-peak baseline measurement with 10 s integration time prior to each measurement session using a 0.05M HNO_3 blank. The measured intensities were then subtracted on line during the analytical sequence for all the samples and standards. Thus, the Kr correction became unnecessary and equations {9} and {10} were not used. The collector configuration of the LGLTPE-2 method (Table 3) allowed the measurement of both ^{91}Zr/^{90}Zr and ^{92}Zr/^{90}Zr ratios. Thus the ^{88}Sr/^{86}Sr ratio could be corrected for mass bias

using the $^{91}Zr/^{90}Zr$ and $^{92}Zr/^{90}Zr$ ratios with equations {6} and {7}, using *True($^{92}Zr/^{90}Zr$)* of 0.333243 (Meija et al., 2016). It was observed by Liu and collaborators that best fit occurred between the mass bias affecting $^{92}Zr/^{90}Zr$ and $^{88}Sr/^{86}Sr$ ratios, compared to that affecting $^{91}Zr/^{90}Zr$ (Liu et al., 2012). These authors also find a better precision when using the $^{92}Zr/^{90}Zr$ ratio. In the present study, both corrections were compared. Measurements giving $\delta^{88}Sr$ values with differences higher than 0.05 ‰ between the two corrections were not considered. The samples $\delta^{88}Sr$ values given here with the LGLTPE-2 method are the $\delta^{88}Sr$ values corrected with the $^{92}Zr/^{90}Zr$ ratio. SSB was also applied using equation {8}. Specificities of each method are summarized in Table 3.

2.5. U (k=2) Expanded uncertainties

The measurement uncertainties in this work regarding certified reference materials are given as expanded uncertainties (U) to compare with other studies. The measurement uncertainties were calculated by multiplying the combined uncertainty $u_c(y)$ of isotopic ratios by a coverage factor k such that $U=ku_c(y)$. Here k=2, which corresponds to a level of confidence of 95 %. The calculation of the combined uncertainty $u_c(y)$ of a δ value involves the uncertainties of the isotopic ratios of the sample and those of the bracketing standards. The full description of the calculation is presented in Sullivan et al. (Sullivan et al., 2020), and the final equation is given here for a symbolic rA/a isotope ratio:

$$u^2(r^{A/a}) = \left(\frac{1}{r_{std}^{A/a}}\right)^2 \times u^2\left(r_{std}^{A/a}\right) + \left(-\frac{r_{spl}^{A/a}}{(r_{std}^{A/a})^2}\right)^2 \times u^2\left(r_{spl}^{A/a}\right) \quad \{10\}$$

With *std* and *spl* corresponding to the standard and the sample, respectively, and *u(r)* the standard uncertainty for the measured ratio, which can be estimated by using the standard deviation calculated from the different blocks corresponding to one block of measurement.

3. Results

3.1. Reference materials

Sample-standard bracketing and the Sr correction methods described produced an $^{87}Sr/^{86}Sr$ ratio for SRM-987 of 0.71023 ± 0,00003 (U, k=2, n=47) at UJ, 0.71037 ± 0.00005 (U, k=2, n=152) for LGLTPE-1 and 0.71026 ± 0.00004 (U, k=2, n=284) for LGLTPE-2 (note again that the commonly used $^{87}Sr/^{86}Sr$ value is 0.71024 ± 0.00026 (McArthur et al., 2015; Weber et al., 2018; Brazier et al., 2019), while the certified value is 0.71034 ± 0.00026). Using the sample-standard bracketing and Zr correction methods, the corresponding SRM-987 $\delta^{88}Sr$ values are -0.003 ± 0.039 ‰ (U, k=2, n=47) at UJ, 0.001 ± 0.094 ‰ (U, k=2, n=152) for LGLTPE-1 and -0.001 ± 0.039 ‰ (U, k=2, n=284) for LGLTPE-2. The $\delta^{88}Sr$ results for the SRM-987 are summarized in Figure S4. The analytical uncertainties in the LGLTPE show a clear improvement when using the LGLTPE-2 method. All the uncertainties are comparable with those measured by TIMS i.e. between 0.026 and 0.074 ‰, U, k=2 (Brazier et al., 2019).

The $\delta^{88}Sr$ values of the fourteen reference materials are presented in Figure 1 and compared with the literature values in Table S3. All literature values used for compilation are presented in Table S4. For the sake of visibility, only some of them are presented in Table S3.

For all standards except UB-N, the results from WIGL-UJ, LGLTPE-1 and LGLTPE-2 are identical within uncertainties. There is a good accuracy with literature values, even for less studied materials such as SRM-1400, SRM-1486, BCR-380R, BCR-383, SRM-1570a, BCR-1 and GS-N. The U (k=2) uncertainties calculated in the present study range between 0.04 and 0.09 ‰. The measured values for UB-N are highly variable, and this variability can be found in the literature, as Brazier et al. (Brazier et al., 2019) and Ma et al. (Ma et al., 2013) are each finding different $\delta^{88}Sr$ values (0.389 ‰ and 0.539 ‰ respectively), suggesting that UB-N is a heterogeneous material.

Radiogenic Sr results for the fourteen reference materials are presented and compared to literature values in Table S5 and all literature values used for compilation are presented in Table S4. For all samples, the results of the present study are in good agreement with referenced values. The expanded uncertainty U (k=2) on the $^{87}Sr/^{86}Sr$ ratio ranges between $3*10^{-5}$ and $6*10^{-5}$, which is slightly higher than that achieved by TIMS ($2*10^{-5}$, (Brazier et al., 2019)).

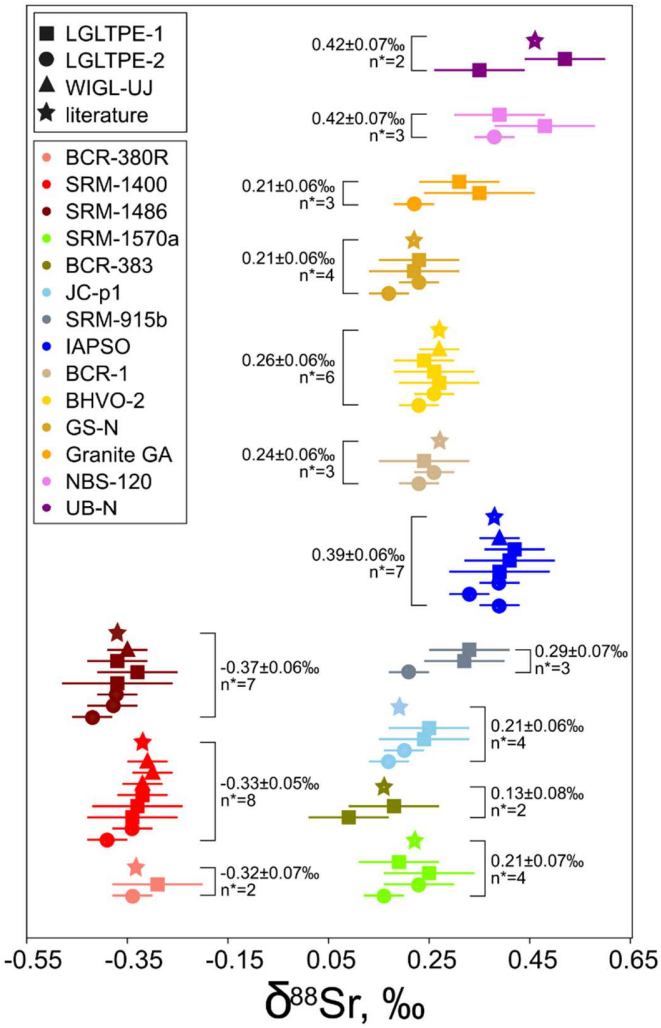

Figure 1: *$\delta^{88}Sr$ values for the reference materials measured in the WIGL-UJ and in the LGLTPE; Error associated to the mean value is the mean of U (k = 2) for each aliquot digested and processed according to the chromatographic procedure. The n* value corresponds to the number of these aliquots. A mean of literature values is presented, all references used for the compilation are presented in Table S2.*

3.2. Tooth enamel samples

The $\delta^{88}Sr$ values and $^{87}Sr/^{86}Sr$ ratios of baboon teeth are given in Table S1. All the samples from baboon teeth were analyzed only once, using the WIGL-UJ method. The mean $\delta^{88}Sr$ value for all first molars of adult baboons is -0.31 ‰. Males (-0.30 ± 0.01 ‰, 2SD, n=2) and females (-0.31 ± 0.02 ‰, 2SD, n=3) have similar $\delta^{88}Sr$ values. The mean $\delta^{88}Sr$ value of all the first molars (adult and young specimens) is -0.32 ± 0.06 ‰ (2SD, n=10). The three deciduous teeth $\delta^{88}Sr$ values are -0.55 ‰ (deciduous incisor), -0.43 ‰ (deciduous premolar), and -0.35 ‰ (deciduous canine). These are significantly lower than first molars $\delta^{88}Sr$ of both adult and young specimens. The third molar has a $\delta^{88}Sr$ value of -0.26 ‰, which is significantly higher than first molars and deciduous teeth. These results are shown in Figure 2A according to the tooth eruption order in baboon life. The $^{87}Sr/^{86}Sr$ values for the ten baboon specimens are presented in Figure 2B. There appears to be three significantly different clusters of specimens. Six specimens with high $^{87}Sr/^{86}Sr$ values (0.722 to 0.721), three adult females with low values (0.719) and one adult male with a very low value (0.716).

The $\delta^{88}Sr$ values and $^{87}Sr/^{86}Sr$ ratios of KNP and WC animals are given in Table S2 and shown in Figure 3 according to species. They were all obtained using the LGLTPE-2 method. The $\delta^{88}Sr$ values range from -0.52 to -0.21 ‰ in enamel and from -0.28 to -0.02 ‰ in plant. At KNP, the mean $\delta^{88}Sr$ value for herbivores is -0.45 ± 0.17 ‰ (2SD, n=11) and is -0.39 ± 0.07 ‰ (2SD, n=5) for carnivores. At WC, there is one herbivorous specimen only (*Tragelaphus scriptus)* and its $\delta^{88}Sr$ value is -0.45 ‰, indistinguishable from the mean $\delta^{88}Sr$ value of *Panthera Leo*, which is -0.44 ± 0.10 ‰ (2SD, n=5). The $^{87}Sr/^{86}Sr$ ratios range from

393 0.707 to 0.760 at KNP and from 0.709 to 0.730 at WC and are consistent with previous
394 results (Balter et al., 2008). This variation range is important and can be explained by the
395 complex geological context of these regions (Schutte, 1986; Shone and Booth, 2005).
396

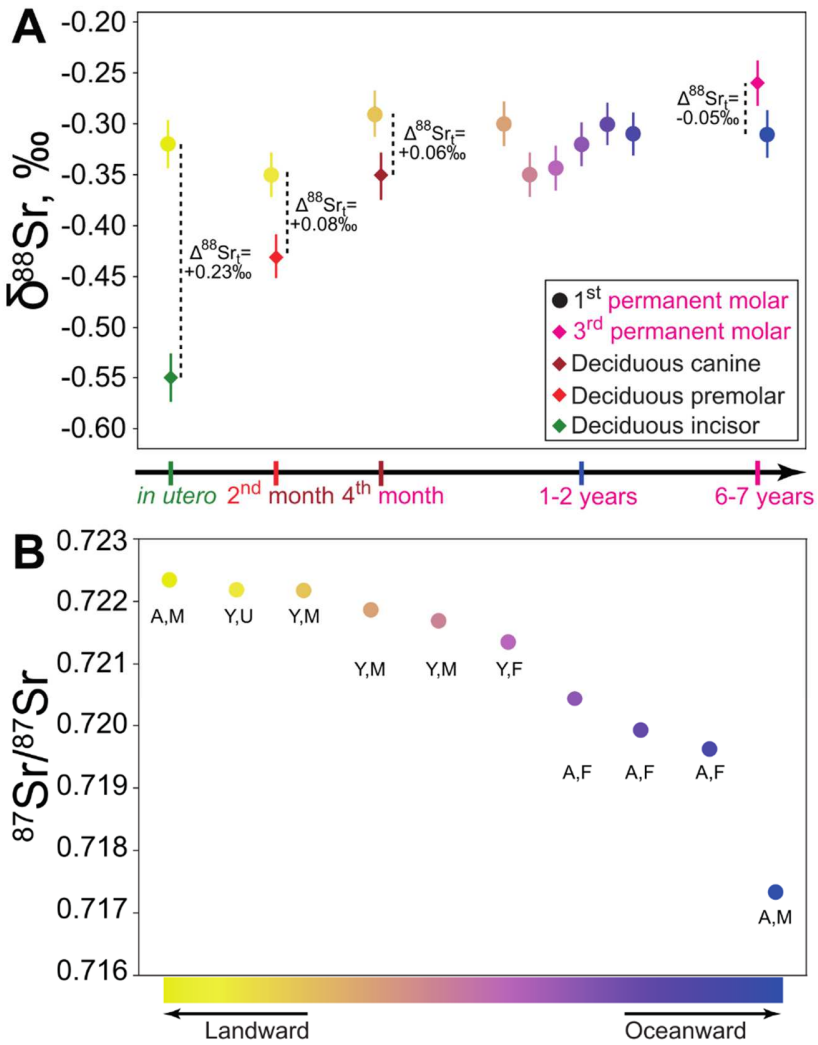

Figure 2: ***A*** *$\delta^{88}Sr$ results of the set of various teeth from the baboon skulls with their erupting order (note that for specimen with both deciduous tooth and 1st permanent molar analyzed, the result for the 1st permanent molar is not presented according to the timeline). Error bars are the 2SD calculated from repeated measurements of the SRM1400 during the same analytical session (0.02 ‰; 2SD; n=4); $\Delta^{88}Sr_t$ is defined for a given specimen as the difference between $\delta^{88}Sr$ value in the first molar and $\delta^{88}Sr$ value in another tooth.* ***B*** *$^{87}Sr/^{86}Sr$ results for 10 baboon specimens; A = adult, Y = young, F = female, M = male, U = unknown sex; The color gradient for1st molars identifies individuals in panel 2A and 2B.*

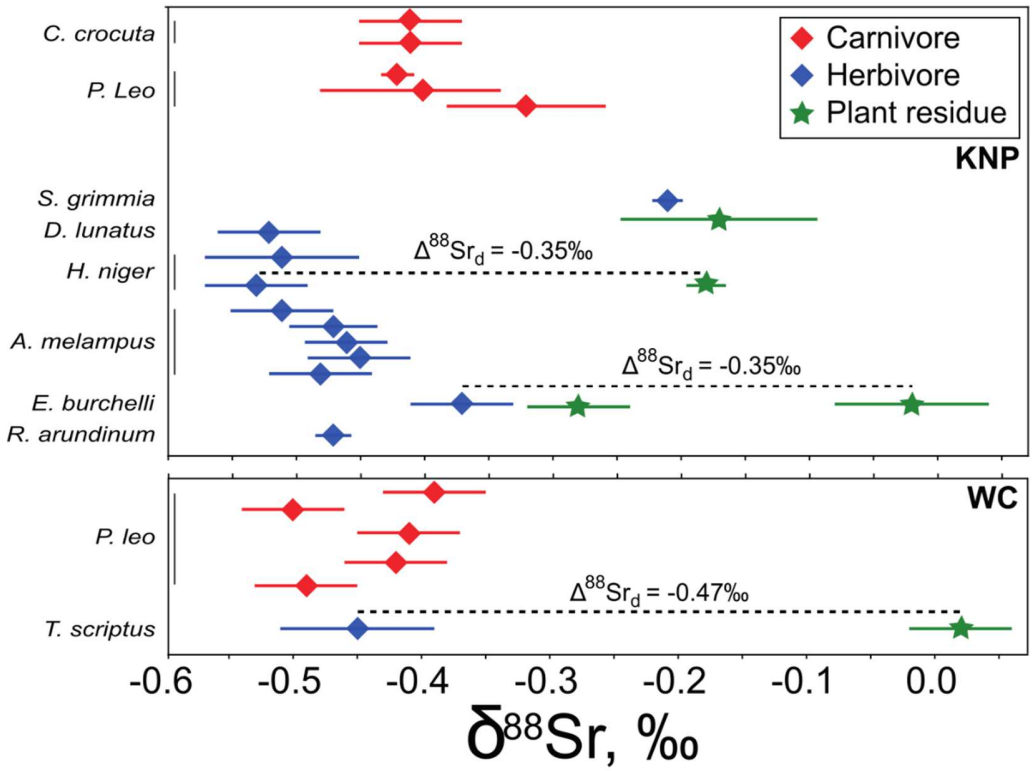

406

407 *Figure 3: $\delta^{88}Sr$ values for carnivores, herbivores and plants in KNP and WC; A dashed line links*

408 *teeth and associated plant residues; The corresponding Sr isotope fractionation value ($\Delta^{88}Sr_d$)*

409 *is given; Errors bars are 2SD calculated on repeated measurements of the same sample*

4. Discussion

4.1. Strontium isotopes in reference materials

Despite small differences between the WIGL-UJ, LGLTPE-1 and LGLTPE-2 methods, notably in the chromatographic separation of Sr (Table 2) and the instrumental settings (Table 3), the $\delta^{88}Sr$ values of reference materials show excellent reproducibility between methods and very good accuracy when compared with literature values. This suggest that the overall protocol is robust, however several observations can be made for some analytical procedures. Consistent with the literature (Liu et al., 2012; Xu et al., 2020), the LGLTPE-2 method using the $^{92}Zr/^{90}Zr$ ratio to correct the instrumental mass bias on $^{88}Sr/^{86}Sr$ shows an enhanced accuracy with literature results (mean accuracy of 0.013 ‰ compared to (Krabbenhöft et al., 2009; Ma et al., 2013; Liu et al., 2017; Brazier et al., 2019)), than the LGLTPE-1 using $^{91}Zr/^{90}Zr$ ratio (mean accuracy of 0.018 ‰ compared to (Krabbenhöft et al., 2009; Ma et al., 2013; Liu et al., 2017; Brazier et al., 2019)). The precision and accuracy at UJ (mean 2SD of 0.02 ‰, and mean accuracy of 0.015 ‰ compared to (Ma et al., 2013; Brazier et al., 2019)) are comparable to those achieved using LGLTPE-2 (mean 2SD of 0.04 ‰, and mean accuracy of 0.013 ‰), showing the importance of the on-peak baseline measurement with systematic blank subtraction. This was not done using LGLTPE-1 and clearly improves the precision of the results and lower the instrumental uncertainties (U(k=2) = 0.09 ‰ for LGLTPE-1 vs U(k=2) = 0.04 ‰ for LGLTPE-2 and UJ). The present results agree very well with the literature, which highlights a clear offset towards ^{88}Sr-depleted biological materials originating from animals (Brazier et al., 2019). To the best of our knowledge, three reference materials studied here had not

been analyzed for strontium isotopes. The SRM-915b is a calcium carbonate standard used in analyses of Ca stable isotopes. It has been measured in three different aliquots, and the mean of its $^{87}Sr/^{86}Sr$ ratio is 0.70800 ± 0.00005 (2SD, n=3). The mean $\delta^{88}Sr$ value is 0.33 ± 0.01 ‰ (2SD, n=2) using the LGLTPE-1 method and 0.21 ‰ using the LGLTPE-2 method. Further measurements are needed to resolve this discrepancy, but we emphasize that the LGLTPE-2 mean is most probably closer to the true value. The NBS-120c is a phosphorite rock, which has been measured in three different aliquots yielding a mean $^{87}Sr/^{86}Sr$ ratio of 0.70885 ± 0.00005 (2SD, n=3) and a mean $\delta^{88}Sr$ value of 0.41 ± 0.06 ‰ (2SD, n=3). Once again, the dispersion between LGLTPE-1 and LGLTPE-2 is quite high. It must be noted that this material shows the highest $\delta^{88}Sr$ value measured in this study. It may be linked with its phosphate nature. Granite GA is a geochemical reference sample of granite material. It has been measured in three different aliquots, yielding a mean $^{87}Sr/^{86}Sr$ value of 0.71376 ± 0.00005 (2SD, n=3). The mean $\delta^{88}Sr$ value measured using LGLTPE-1 is 0.33 ± 0.04 ‰ (2SD, n=2) and the one measured using LGLTPE-2 is 0.22 ± 0.03 ‰. Further measurements are needed to choose between these two values, but the LGLTPE-2 mean is most probably closer to the actual value. As the measurement method is shown to be reliable using reference materials, it is possible to interpret the results obtained on biological material such as plant and tooth enamel.

4.2. Intra-individual variations of enamel Sr isotopes

The study of different tooth types in modern baboons allows evaluation of the extent of intra-individual variations of the $\delta^{88}Sr$ value. Of note is that all the baboon teeth have negative $\delta^{88}Sr$ values, in accordance with available data for bone and teeth (Knudson et al.,

2010; Romaniello et al., 2015; Lewis et al., 2017; Brazier et al., 2019). Discussion on the possible use of the $\delta^{88}Sr$ value as a dietary proxy is challenging for baboons because there is a lack of isotopic data for possible dietary sources, which could be numerous as these are omnivorous animals (Hamilton III et al., 1978; Codron et al., 2006; Johnson et al., 2013). The most obvious pattern is a clear difference between the $\delta^{88}Sr$ value of milk and permanent teeth, the latter being ^{88}Sr-enriched compared to the former. This indicates a difference of diet between baboons older than six years old and baboons younger than four. The most likely explanation is that young baboons consume breast milk in various but decreasing amounts during their first years. It is known that the Sr/Ca ratio is much lower in breast milk than in other non-milk foods (Sillen and Smith, 1984; Mays, 2003; Humphrey et al., 2008; Nava et al., 2020). This difference between milk and non-milk food is explained by bio-purification processes, discriminating Sr against Ca in the mother's body. For instance, Ca is preferentially transferred across the mammary gland during lactation, whereas the circulation of Sr is passively constrained by the concentration gradient (Tsutaya and Yoneda, 2015). This process is known to also induce a mass-dependent fractionation of Ca isotopes, where milk is ^{44}Ca-depleted. The resulting negative $\delta^{44/42}Ca$ signature and lower Sr/Ca ratio is found in human deciduous teeth and yields information about lactation period and weaning processes in modern and ancient human population (Tacail et al., 2017, 2019; Li et al., 2020).

The present $\delta^{88}Sr$ results suggest that Sr isotopes may also undergo mass-fractionation through mammary glands leading to a ^{88}Sr-depleted breast milk, compared to non-milk food and can trace the intensity of breast feeding and duration of the weaning process. Defining $\Delta^{88}Sr_t$ for one individual as the difference between the $\delta^{88}Sr$ value in the

479 first molar and another tooth, shows decreasing values with increasing age at tooth
480 eruption (Figure 2A). Providing that milk has a low $\delta^{88}Sr$ value, this suggests the declining
481 contribution of milk in baboon's diet as the animal ages. More precisely, during the first
482 two-to-three months of life, young baboons are mostly breastfed and start to include non-
483 milk food after the fourth month, while continuing to consume mother's milk to some
484 extent. After the first year, baboons seem to shift to a milk-free adult diet. These dietary
485 histories are consistent with known weaning processes of baboons (Rhine et al., 1985;
486 Humphrey et al., 2008).

487 The $^{87}Sr/^{86}Sr$ ratios have been measured in the first molars and are distributed
488 according to three groups (Figure 2B) that should represent distinct bedrock types of the
489 WC region. The $^{87}Sr/^{86}Sr$ ratios measured in enamel are consistent with the variability of
490 the bioavailable $^{87}Sr/^{86}Sr$ ratios of plants measured in this area. In this region, the plant
491 $^{87}Sr/^{86}Sr$ value gradually increases from 0.7087 to 0.7242 over 100 km between the coast
492 and the land (Copeland et al., 2016). The baboons $^{87}Sr/^{86}Sr$ values thus indicate that the
493 specimens were not living altogether at the same place when their first molars were
494 forming. The baboons analyzed here originated from two different troops that were killed
495 during hunting for population control in the Calitzdorp area (Brand, 1994). Chacma
496 baboons are known to form sub-troops seasonally (Anderson, 1981), which are composed
497 of a majority of adult females and young baboons (Anderson, 1981; Busse, 1984; Henzi et
498 al., 1999). While it is not possible to reallocate baboon individuals in one or the other troop,
499 our results however suggest that the $^{87}Sr/^{86}Sr$ ratio in enamel can help to reconstitute sub-
500 trooping recruitment strategies in living primates.

501

4.3. Inter-individual variations of enamel Sr isotopes

For individuals found with plant residues, a $\Delta^{88}Sr_d$ can be defined as the difference between $\delta^{88}Sr$ value of the animal and that of the plant (Figure 3). TM16661-PR and TM16690-PR are plant residues from teeth of specimens that were not analyzed in this study. The $\Delta^{88}Sr_d$ is always negative, indicating that the $\delta^{88}Sr$ values of herbivores tooth enamel is ^{88}Sr-depleted relative to plants, consistent with a feeding study performed on pigs (Lewis et al., 2017). These authors found a $\Delta^{88}Sr_d$ value of -0.32±0.06 ‰, close to the average of -0.26 ‰ calculated here. Our results exhibit a much higher dispersion of the $\Delta^{88}Sr_d$ values, which can be explained by the natural, and therefore uncontrolled, context of the study. A Wilcoxson rank test was performed on all the $\delta^{88}Sr$ dataset of KNP to compare results for herbivores and carnivores. The *P*-value obtained is 0.03 suggesting that the differences between herbivores and carnivores can be considered significant. Thus, the $\Delta^{88}Sr_d$ values can also be calculated from enamel of carnivores to herbivores, and are, strikingly, not negative. At KNP, the $\Delta^{88}Sr_d$ value is 0.06 ‰, but it reaches 0.08 ‰ when one possible herbivore outlier (*Sylvicapra grimmia*) is excluded. Indeed, *Sylvicapra grimmia* presents the highest $\delta^{88}Sr$ and $^{87}Sr/^{86}Sr$ values (respectively -0.21 ‰ and 0.760) in the KNP dataset, which suggests a location effect. *Equus burchelli* also presents a higher $\delta^{88}Sr$ value than the other herbivores and represents the only pure grazer in the herbivore set, so different metabolisms may play a role in $\delta^{88}Sr$ differences. In the WC, the $\Delta^{88}Sr_d$ value is 0.01 ‰, but it is a less robust measure due to the presence of only one herbivore. The pattern of the Sr stable isotopes fractionation from plants to carnivores resembles that of Zn, for which the $\delta^{66}Zn$ value first strongly increases from plants to herbivores and then decreases to carnivores (Jaouen et al., 2013). The systematics of Sr stable isotope

fractionation up mammal trophic chain thus requires further investigations to understand the origin of the observed isotopic variability before validating the $\delta^{88}Sr$ value as a robust proxy of past diet and trophic position.

4.4. Further perspectives for combined stable and radiogenic Sr analyses

The present study emphasizes the interest and feasibility of analyzing the $\delta^{88}Sr$ and $^{87}Sr/^{86}Sr$ values simultaneously. Cost and duration of measurement is the same as when analyzing one or the other independently using MC-ICP-MS. The Sr chromatographic separation for 24 samples takes a day only, and with the whole SSB procedure, one sample can be analyzed in 45 minutes. The simplicity of the methodology will surely encourage more studies using stable and radiogenic Sr isotopes for (paleo)ecological and geological purposes.

Other non-traditional stable isotopes are already fulfilling the role of dietary/weaning tracer, such as $\delta^{44/42}Ca$ (Martin et al., 2018; Tacail et al., 2019Tacail et al., 2020, 2021), and $\delta^{66/64}Zn$ (Jaouen et al., 2013, 2016, 2020; Bourgon et al., 2020) measured in the mineral phase (hydroxyapatite) of bone and teeth. So far, the original $\delta^{44/42}Ca$ and $\delta^{66/64}Zn$ signatures are shown to be preserved in tooth enamel hydroxyapatite, (Martin et al., 2015; Hassler et al., 2018; Bourgon et al., 2020). As presented here, the combined $\delta^{88}Sr$ and $^{87}Sr/^{86}Sr$ analyses in animal and vegetal tissues provide information about diet and localization, and thus may enable an extended reconstruction of life history. Further work is needed to assess the preservation of the biological signature of Sr isotopes in fossil bone and tooth enamel. More studies are also needed to decipher the behavior of Sr through

metabolic processes such as digestion or milk production, because metabolism may override the Sr dietary isotopic signature. The $\delta^{88}Sr$ value could represent a metabolic signature of the studied taxa. Results of stable Sr isotopes have been recently obtained by Nitzsche et al. in invertebrates of a stream food web (Nitzsche et al., 2022). The $\delta^{88}Sr$ value seems to discriminate different feeding behaviors and might be a dietary tracer in aquatic as well as terrestrial ecosystems.

The perspectives of $\delta^{88}Sr$ and $^{87}Sr/^{86}Sr$ combined analyses are not restricted to paleo(ecological) studies. A temperature dependent Sr isotope fractionation occurs between water and biologically mineralized carbonates. A 0.033‰/°C thermodependency is reported for natural coral samples (*Pavona clavus*) (Fietzke and Eisenhauer, 2006) and a similar value of 0.026 ‰/°C has been determined for another coral species (*Lophelia pertusa*) (Rüggeberg et al., 2008). A preliminary study shows that there might be a similar thermo-dependent process of fractionation for stable Sr isotopes in coccolithophore species (Stevenson et al., 2014). These studies suggest that the $\delta^{88}Sr$ value in carbonates could be used as a paleothermometer to reconstruct ancient ocean temperatures along with the $^{87}Sr/^{86}Sr$ value that could be used as a time calibration tool (Veizer et al., 1999).

Considering the differences between silicate-dominated (Bulk silicate Earth $\delta^{88}Sr$ value estimated as 0.29 ‰ (Ma et al., 2013)) and carbonate-dominated systems (Marine carbonates $\delta^{88}Sr$ value between 0.10 and 0.20 ‰ (Krabbenhöft et al., 2010)), the measurement of $\delta^{88}Sr$ could be an added value to that of $^{87}Sr/^{86}Sr$ for studying weathering processes. There is a preferential leaching of heavy Sr isotopes into the hydrosphere during silicate weathering, but a preferential leaching of light Sr isotope preferential leaching of

heavy strontium during primary formed carbonate weathering (Chao et al., 2015) . The river $\delta^{88}Sr$ value is therefore different whether it is carbonate- or silicate-dominated and this helps to identify the weathering processes that occurred before the water reached the river. The concomitant analysis of the $^{87}Sr/^{86}Sr$ value could give additional constrains on the provenance of the weathered material.

5. Conclusion

The measurement of Sr stable isotopes by MC-ICPMS using combined sample-standard bracketing and Zr correction is shown to be a robust and easy method. The method permits the simultaneous measurement of the stable $^{88}Sr/^{86}Sr$ and radiogenic $^{87}Sr/^{86}Sr$ ratios. This method has been implemented and evaluated in different laboratories and yields accurate and reproducible results on a wide variety of reference materials. Preliminary results on tooth enamel samples show that the $\delta^{88}Sr$ value is a potential indicator of weaning practices. Encouraging results show that enamel $\delta^{88}Sr$ values potentially discriminate herbivores from carnivores, but this necessitates further studies to understand the source of isotopic heterogeneity. Generally, more data is necessary to better understand the effect of physiology on Sr isotopes and to extend the use of the $\delta^{88}Sr$ values as a companion of $\delta^{44/42}Ca$ in biomedical studies.

Conflicts of interest

There are no conflicts of interest to declare.

Acknowledgements

Many thanks are due to the Ditsong National Museum of Natural History (Pretoria, South Africa), for providing access to the samples. We would like to thank Clément P. Bataille, and an anonymous reviewer for their helpful comments that helped improve the clarity of the paper.

References

Anderson C. M. (1981) Subtrooping in a chacma baboon (Papio ursinus) population. *Primates* **22**, 445–458.

Argentino C., Lugli F., Cipriani A. and Panieri G. (2021) Testing miniaturized extraction chromatography protocols for combined 87Sr/86Sr and δ88/86Sr analyses of pore water by MC-ICP-MS. *Limnol. Oceanogr. Methods* **19**, 431–440.

Balter V. (2004) Allometric constraints on Sr/Ca and Ba/Ca partitioning in terrestrial mammalian trophic chains. *Oecologia* **139**, 83–88.

Balter V., Telouk P., Reynard B., Braga J., Thackeray F. and Albarède F. (2008) Analysis of coupled Sr/Ca and 87Sr/86Sr variations in enamel using laser-ablation tandem quadrupole-multicollector ICPMS. *Geochim. Cosmochim. Acta* **72**, 3980–3990.

Bourgon N., Jaouen K., Bacon A.-M., Jochum K. P., Dufour E., Duringer P., Ponche J.-L., Joannes-Boyau R., Boesch Q., Antoine P.-O., and others (2020) Zinc isotopes in Late Pleistocene fossil teeth from a Southeast Asian cave setting preserve paleodietary information. *Proc. Natl. Acad. Sci.* **117**, 4675–4681.

Brand D. (1994) Weight growth of chacma baboons in the southern Cape province, South Africa. *Rev. Zool. Afr. 1974* **108**, 71–75.

Brazier J.-M., Schmitt A.-D., Pelt E., Lemarchand D., Gangloff S., Tacail T. and Balter V. (2019) Determination of Radiogenic 87Sr/86Sr and Stable δ88/86SrSRM987 Isotope Values of Thirteen Mineral, Vegetal and Animal Reference Materials by DS-TIMS. *Geostand. Geoanalytical Res.*

Busse C. D. (1984) Spatial structure of chacma baboon groups. *Int. J. Primatol.* **5**, 247–261.

619 Chao H.-C., You C.-F., Liu H.-C. and Chung C.-H. (2015) Evidence for stable Sr isotope
620 fractionation by silicate weathering in a small sedimentary watershed in
621 southwestern Taiwan. *Geochim. Cosmochim. Acta* **165**, 324–341.

622 Charlier B., Parkinson I., Burton K., Grady M., Wilson C. and Smith E. (2017) Stable
623 strontium isotopic heterogeneity in the solar system from double-spike data.
624 *Geochem. Perspect. Lett.* **4**, 35–40.

625 Codron D., Lee-Thorp J. A., Sponheimer M., de Ruiter D. and Codron J. (2006) Inter-and
626 intrahabitat dietary variability of chacma baboons (Papio ursinus) in South African
627 savannas based on fecal δ13C, δ15N, and% N. *Am. J. Phys. Anthropol. Off. Publ. Am.*
628 *Assoc. Phys. Anthropol.* **129**, 204–214.

629 Copeland S. R., Cawthra H. C., Fisher E. C., Lee-Thorp J. A., Cowling R. M., Le Roux P. J.,
630 Hodgkins J. and Marean C. W. (2016) Strontium isotope investigation of ungulate
631 movement patterns on the Pleistocene Paleo-Agulhas plain of the Greater Cape
632 floristic region, South Africa. *Quat. Sci. Rev.* **141**, 65–84.

633 De Muynck D., Huelga-Suarez G., Van Heghe L., Degryse P. and Vanhaecke F. (2009)
634 Systematic evaluation of a strontium-specific extraction chromatographic resin for
635 obtaining a purified Sr fraction with quantitative recovery from complex and Ca-rich
636 matrices. *J. Anal. At. Spectrom.* **24**, 1498–1510.

637 Ehrlich S., Gavrieli I., Dor L.-B. and Halicz L. (2001) Direct high-precision measurements of
638 the 87Sr/86Sr isotope ratio in natural water, carbonates and related materials by
639 multiple collector inductively coupled plasma mass spectrometry (MC-ICP-MS). *J.*
640 *Anal. At. Spectrom.* **16**, 1389–1392.

641 Ericson J. E. (1985) Strontium isotope characterization in the study of prehistoric human
642 ecology. *J. Hum. Evol.* **14**, 503–514.

643 Fietzke J. and Eisenhauer A. (2006) Determination of temperature-dependent stable
644 strontium isotope (88Sr/86Sr) fractionation via bracketing standard MC-ICP-MS.
645 *Geochem. Geophys. Geosystems* **7**.

646 Guibourdenche L., Stevenson R., Pedneault K., Poirier A. and Widory D. (2020)
647 Characterizing nutrient pathways in Quebec (Canada) vineyards: Insight from stable
648 and radiogenic strontium isotopes. *Chem. Geol.* **532**, 119375.

649 Hajj F., Poszwa A., Bouchez J. and Guérold F. (2017) Radiogenic and “stable” strontium
650 isotopes in provenance studies: A review and first results on archaeological wood
651 from shipwrecks. *J. Archaeol. Sci.* **86**, 24–49.

652 Hamilton III W. J., Buskirk R. E. and Buskirk W. H. (1978) Omnivory and utilization of food
653 resources by chacma baboons, Papio ursinus. *Am. Nat.* **112**, 911–924.

Hassler A., Martin J. E., Amiot R., Tacail T., Godet F. A., Allain R. and Balter V. (2018) Calcium isotopes offer clues on resource partitioning among Cretaceous predatory dinosaurs. *Proc. R. Soc. B Biol. Sci.* **285**, 20180197.

Henzi S., Weingrill T. and Barrett L. (1999) Male behaviour and the evolutionary ecology of chacma baboons. *South Afr. J. Sci.* **95**, 240–242.

Humphrey L. T., Dirks W., Dean M. C. and Jeffries T. E. (2008) Tracking dietary transitions in weanling baboons (Papio hamadryas anubis) using strontium/calcium ratios in enamel. *Folia Primatol. (Basel)* **79**, 197–212.

Irrgeher J., Prohaska T., Sturgeon R. E., Mester Z. and Yang L. (2013) Determination of strontium isotope amount ratios in biological tissues using MC-ICPMS. *Anal. Methods* **5**, 1687–1694.

Jaouen K., Beasley M., Schoeninger M., Hublin J.-J. and Richards M. P. (2016) Zinc isotope ratios of bones and teeth as new dietary indicators: results from a modern food web (Koobi Fora, Kenya). *Sci. Rep.* **6**, 26281.

Jaouen K., Pons M.-L. and Balter V. (2013) Iron, copper and zinc isotopic fractionation up mammal trophic chains. *Earth Planet. Sci. Lett.* **374**, 164–172.

Jaouen K., Trost M., Bourgon N., Colleter R., Le Cabec A., Tütken T., Elias Oliveira R., Pons M. L., Méjean P., Steinbrenner S., and others (2020) Zinc isotope variations in archeological human teeth (Lapa do Santo, Brazil) reveal dietary transitions in childhood and no contamination from gloves. *PloS One* **15**, e0232379.

Johnson C. A., Raubenheimer D., Rothman J. M., Clarke D. and Swedell L. (2013) 30 days in the life: daily nutrient balancing in a wild chacma baboon. *PLoS One* **8**.

Knudson K. J., Price T. D., Buikstra J. E. and Blom D. E. (2004) The use of strontium isotope analysis to investigate Tiwanaku migration and mortuary ritual in Bolivia and Peru. *Archaeometry* **46**, 5–18.

Knudson K. J., Williams H. M., Buikstra J. E., Tomczak P. D., Gordon G. W. and Anbar A. D. (2010) Introducing δ88/86Sr analysis in archaeology: a demonstration of the utility of strontium isotope fractionation in paleodietary studies. *J. Archaeol. Sci.* **37**, 2352–2364.

Krabbenhöft A., Eisenhauer A., Böhm F., Vollstaedt H., Fietzke J., Liebetrau V., Augustin N., Peucker-Ehrenbrink B., Müller M., Horn C., and others (2010) Constraining the marine strontium budget with natural strontium isotope fractionations (87Sr/86Sr, δ88/86Sr) of carbonates, hydrothermal solutions and river waters. *Geochim. Cosmochim. Acta* **74**, 4097–4109.

Krabbenhöft A., Fietzke J., Eisenhauer A., Liebetrau V., Böhm F. and Vollstaedt H. (2009) Determination of radiogenic and stable strontium isotope ratios (87 Sr/86 Sr; δ

88/86 Sr) by thermal ionization mass spectrometry applying an 87 Sr/84 Sr double spike. *J. Anal. At. Spectrom.* **24**, 1267–1271.

Lazzerini N., Balter V., Coulon A., Tacail T., Marchina C., Lemoine M., Bayarkhuu N., Turbat T., Lepetz S. and Zazzo A. (2021) Monthly mobility inferred from isoscapes and laser ablation strontium isotope ratios in caprine tooth enamel. *Sci. Rep.* **11**, 2277.

Lewis J., Pike A., Coath C. and Evershed R. (2017) Strontium concentration, radiogenic (87Sr/86Sr) and stable (δ 88Sr) strontium isotope systematics in a controlled feeding study. *STAR Sci. Technol. Archaeol. Res.* **3**, 45–57.

Li Q., Nava A., Reynard L. M., Thirlwall M., Bondioli L. and Müller W. (2020) Spatially-Resolved Ca Isotopic and Trace Element Variations in Human Deciduous Teeth Record Diet and Physiological Change. *Environ. Archaeol.*, 1–10.

Liu H.-C., Chung C.-H., You C.-F. and Chiang Y.-H. (2016) Determination of 87 Sr/86 Sr and δ 88/86 Sr ratios in plant materials using MC-ICP-MS. *Anal. Bioanal. Chem.* **408**, 387–397.

Liu H.-C., You C.-F., Huang K.-F. and Chung C.-H. (2012) Precise determination of triple Sr isotopes (δ87Sr and δ88Sr) using MC-ICP-MS. *Talanta* **88**, 338–344.

Liu H.-C., You C.-F., Zhou H., Huang K.-F., Chung C.-H., Huang W.-J. and Tang J. (2017) Effect of calcite precipitation on stable strontium isotopic compositions: Insights from riverine and pool waters in a karst cave. *Chem. Geol.* **456**, 85–97.

Ma J., Wei G., Liu Y., Ren Z., Xu Y. and Yang Y. (2013) Precise measurement of stable (δ 88/86 Sr) and radiogenic (87 Sr/86 Sr) strontium isotope ratios in geological standard reference materials using MC-ICP-MS. *Chin. Sci. Bull.* **58**, 3111–3118.

Maréchal C. N., Télouk P. and Albarède F. (1999) Precise analysis of copper and zinc isotopic compositions by plasma-source mass spectrometry. *Chem. Geol.* **156**, 251–273.

Marisa Almeida C. and D. Vasconcelos M. T. S. (2001) ICP-MS determination of strontium isotope ratio in wine in order to be used as a fingerprint of its regional origin. *J. Anal. At. Spectrom.* **16**, 607–611.

Martin J. E., Tacail T., Adnet S., Girard C. and Balter V. (2015) Calcium isotopes reveal the trophic position of extant and fossil elasmobranchs. *Chem. Geol.* **415**, 118–125.

Mays S. (2003) Bone strontium: calcium ratios and duration of breastfeeding in a Mediaeval skeletal population. *J. Archaeol. Sci.* **30**, 731–741.

McArthur J. M., Howarth R. J. and Bailey T. R. (2015) Strontium Isotope Stratigraphy: LOWESS Version 3: Best Fit to the Marine Sr-Isotope Curve for 0–509 Ma and Accompanying Look-up Table for Deriving Numerical Age. *J. Geol.*

724 Meija J., Coplen T. B., Berglund M., Brand W. A., De Bièvre P., Gröning M., Holden N. E.,
725 Irrgeher J., Loss R. D., Walczyk T., and others (2016) Atomic weights of the elements
726 2013 (IUPAC Technical Report). *Pure Appl. Chem.* **88**, 265–291.

727 Nava A., Lugli F., Romandini M., Badino F., Evans D., Helbling A. H., Oxilia G., Arrighi S.,
728 Bortolini E., Delpiano D., Duches R., Figus C., Livraghi A., Marciani G., Silvestrini S.,
729 Cipriani A., Giovanardi T., Pini R., Tuniz C., Bernardini F., Dori I., Coppa A., Cristiani E.,
730 Dean C., Bondioli L., Peresani M., Müller W. and Benazzi S. (2020) Early life of
731 Neanderthals. *Proc. Natl. Acad. Sci.* **117**, 28719–28726.

732 Neymark L. A., Premo W. R., Mel'nikov N. N. and Emsbo P. (2014) Precise determination of δ
733 88 Sr in rocks, minerals, and waters by double-spike TIMS: a powerful tool in the
734 study of geological, hydrological and biological processes. *J. Anal. At. Spectrom.* **29**,
735 65–75.

736 Nitzsche K. N., Wakaki S., Yamashita K., Shin K.-C., Kato Y., Kamauchi H. and Tayasu I. (2022)
737 Calcium and strontium stable isotopes reveal similar behaviors of essential Ca and
738 nonessential Sr in stream food webs. *Ecosphere* **13**, e3921.

739 Ohno T. and Hirata T. (2007) Simultaneous determination of mass-dependent isotopic
740 fractionation and radiogenic isotope variation of strontium in geochemical samples
741 by multiple collector-ICP-mass spectrometry. *Anal. Sci.* **23**, 1275–1280.

742 Price T. D., Burton J. H. and Bentley R. A. (2002) The Characterization of Biologically
743 Available Strontium Isotope Ratios for the Study of Prehistoric Migration.
744 *Archaeometry* **44**, 117–135.

745 Rhine R., Norton G., Wynn G. and Wynn R. (1985) Weaning of free-ranging infant baboons
746 (Papio cynocephalus) as indicated by one-zero and instantaneous sampling of
747 feeding. *Int. J. Primatol.* **6**, 491.

748 Romaniello S., Field M., Smith H., Gordon G., Kim M. and Anbar A. (2015) Fully automated
749 chromatographic purification of Sr and Ca for isotopic analysis. *J. Anal. At. Spectrom.*
750 **30**, 1906–1912.

751 Rüggeberg A., Fietzke J., Liebetrau V., Eisenhauer A., Dullo W.-C. and Freiwald A. (2008)
752 Stable strontium isotopes (δ88/86Sr) in cold-water corals—a new proxy for
753 reconstruction of intermediate ocean water temperatures. *Earth Planet. Sci. Lett.*
754 **269**, 570–575.

755 Russell W., Papanastassiou D. and Tombrello T. (1978) Ca isotope fractionation on the
756 Earth and other solar system materials. *Geochim. Cosmochim. Acta* **42**, 1075–1090.

757 Schutte I. (1986) The general geology of the Kruger National Park. *Koedoe Afr. Prot. Area*
758 *Conserv. Sci.*

759 Shone R. W. and Booth P. W. K. (2005) The Cape Basin, South Africa: A review. *J. Afr. Earth*
760 *Sci.* **43**, 196–210.

761 Sillen A., Hall G., Richardson S. and Armstrong R. (1998) 87Sr/86Sr ratios in modern and
762 fossil food-webs of the Sterkfontein Valley: implications for early hominid habitat
763 preference. *Geochim. Cosmochim. Acta* **62**, 2463–2473.

764 Sillen A. and Smith P. (1984) Weaning patterns are reflected in strontium-calcium ratios of
765 juvenile skeletons. *J. Archaeol. Sci.* **11**, 237–245.

766 de Souza G. F., Reynolds B. C., Kiczka M. and Bourdon B. (2010) Evidence for mass-
767 dependent isotopic fractionation of strontium in a glaciated granitic watershed.
768 *Geochim. Cosmochim. Acta* **74**, 2596–2614.

769 Stevenson E. I., Hermoso M., Rickaby R. E., Tyler J. J., Minoletti F., Parkinson I. J., Mokadem F.
770 and Burton K. W. (2014) Controls on stable strontium isotope fractionation in
771 coccolithophores with implications for the marine Sr cycle. *Geochim. Cosmochim.*
772 *Acta* **128**, 225–235.

773 Sullivan K., Layton-Matthews D., Leybourne M., Kidder J., Mester Z. and Yang L. (2020)
774 Copper Isotopic Analysis in Geological and Biological Reference Materials by MC-
775 ICP-MS. *Geostand. Geoanalytical Res.* **44**, 349–362.

776 Tacail T., Albalat E., Télouk P. and Balter V. (2014) A simplified protocol for measurement of
777 Ca isotopes in biological samples. *J. Anal. At. Spectrom.* **29**, 529–535.

778 Tacail T., Martin J. E., Arnaud-Godet F., Thackeray J. F., Cerling T. E., Braga J. and Balter V.
779 (2019) Calcium isotopic patterns in enamel reflect different nursing behaviors
780 among South African early hominins. *Sci. Adv.* **5**, eaax3250.

781 Tacail T., Thivichon-Prince B., Martin J. E., Charles C., Viriot L. and Balter V. (2017) Assessing
782 human weaning practices with calcium isotopes in tooth enamel. *Proc. Natl. Acad.*
783 *Sci.* **114**, 6268–6273.

784 Tsutaya T. and Yoneda M. (2015) Reconstruction of breastfeeding and weaning practices
785 using stable isotope and trace element analyses: A review. *Am. J. Phys. Anthropol.*
786 **156**, 2–21.

787 Veizer J., Ala D., Azmy K., Bruckschen P., Buhl D., Bruhn F., Carden G. A. F., Diener A., Ebneth
788 S., Godderis Y., Jasper T., Korte C., Pawellek F., Podlaha O. G. and Strauss H. (1999)
789 87Sr/86Sr, δ13C and δ18O evolution of Phanerozoic seawater. *Chem. Geol.* **161**, 59–
790 88.

791 Weber M., Lugli F., Jochum K. P., Cipriani A. and Scholz D. (2018) Calcium Carbonate and
792 Phosphate Reference Materials for Monitoring Bulk and Microanalytical
793 Determination of Sr Isotopes. *Geostand. Geoanalytical Res.* **42**, 77–89.

794 Xu J., Yang S., Yang Y., Liu Y., Xie X. and Spectroscopy A. (2020) Precise Determination of
795 Stable Strontium Isotopic Compositions by MC-ICP-MS. *At. Spectrosc. -Norwalk Conn.*
796 **41**, 64–73.

797